ELSEVIER

Journal of Alloys and Compounds 404–406 (2005) 473–476

Journal of ALLOYS AND COMPOUNDS

www.elsevier.com/locate/jallcom

Hydrogen electrosorption and structural properties of nanostructured Pd–Mg thin films elaborated by pulsed laser deposition

J. Paillier, L. Roue*

I.N.R.S.-Énergie, Matériaux and Télécommunications, 1650 Bld. Lionel Boulet, Varennes (PQ), Canada J3X 1S2

Received 19 May 2004; received in revised form 2 November 2004; accepted 12 November 2004
Available online 14 July 2005

Abstract

Mg–Pd films with different morphologies were prepared using the pulsed laser deposition (PLD) technique. Their structure and electrochemical hydriding behaviour were investigated. The gas (Ar or He) introduced into the PLD chamber has a strong influence on the resulting film structure. Mg films without MgO are obtained when using Ar or He gas at around 350 mTorr. The most promising geometry is obtained under He pressure and consists of a Pd-coated magnesium film with an extended Pd–Mg mixing region, which may increase the number of Pd–Mg interfaces. This film displays remarkable electrochemical hydriding properties in KOH solution.

Keywords: Hydrogen storage material; Magnesium; Palladium; Thin film; Pulsed laser deposition

1. Introduction

Multi-layered Pd/Mg films prepared by RF-sputtering display remarkable hydrogen storage properties (5 wt.% in Mg at 373 K and 0.1 MPa) due to cooperative phenomena in nano-composite interface regions between the Pd and Mg layers [1–3]. We report hereafter the structural and electrochemical hydriding properties of nanostructured Pd–Mg films synthesized by means of pulsed laser deposition (PLD). The PLD technique differs from quite common deposition techniques such as sputtering or evaporation in two main features [4]: (i) the high energy of the ejected species (i.e. the ablated species are a mix of ions in the keV range and neutral atoms with energies of several eV); (ii) the discontinuity of the deposition process (i.e. periods of some nanoseconds of target ablation are alternated with longer periods |10 ms at 100 Hz| of non-ablation). This gives high instantaneous deposition rate (several kÅ/s) and favours the formation of non-equilibrium films. Moreover, its flexibility in use allows the synthesis of multi-layered films.

2. Experimental

Depositions were performed at room temperature using a pulsed KrF excimer laser ($\lambda = 248$ nm, pulse width = 20 ns, repetition rate = 100 Hz) with a laser fluence of 5 J cm^{-2}. Prior the deposition, the chamber was evacuated to a pressure of about 10^{-3} Pa. The targets for ablation were Pd and Mg foils (99.9%; Alfa Æsar). Three types of films were prepared: (i) film 1: a layer of Pd was deposited onto a coarse-grained Mg substrate. No gas was introduced into the chamber; (ii) film 2: in the presence of argon (350 mTorr $=\sim$ 47 Pa), the Mg film was deposited on a coarse-grained Ni substrate and covered by a Pd layer; (iii) film 3: in the presence of helium (350 mTorr), the Mg film was deposited on a coarse-grained Ni substrate and covered by a Pd layer.

X-ray diffraction (XRD) was done using a Bruker D8 diffractometer with Cu Kα radiation and a fixed grazing angle of 2°. The thickness of the films was measured by Rutherford backscattering spectrometry (RBS) with 350 keV He^{++}. Depth profiles were obtained from XPS measurements performed on a VG Escalab 220I-XL with an Al Kα monochromatic source and using Ar^{+} ion sputtering (5 keV, 0.1 μA). Electrochemical experiments were performed

* Corresponding author. Tel.: +1 450 929 8214; fax: +1 450 929 8102.
E-mail address: roue@emt.inrs.ca (L. Roue).

0925-8388/$ – see front matter © 2005 Elsevier B.V. All rights reserved.
doi:10.1016/j.jallcom.2004.11.119

at room temperature in 1 M KOH solution with a three-electrode cell using a Voltalab40 potentiostat/galvanostat. The counter electrode was a Pt wire and the reference electrode was an Hg/HgO electrode.

3. Results and discussion

3.1. Structure

3.1.1. Film 1

The sample consists of a palladium layer deposited on a polycrystalline Mg substrate. Its thickness is 27 nm. XRD analysis confirms that the film is constituted of a single Pd phase (see Fig. 1a). The Pd crystallite size determined using the Scherrer formula is ∼10 nm. No texture is observed. The lattice of the Pd layer presents strong and anisotropic strains ($\varepsilon_{111} = +1.8\%$, $\varepsilon_{100} = +2.8\%$). It is assumed that strong stresses were created during the film growth by the crystallite coalescence process. Such a mechanism is known to create stresses of several GPa when the adatoms mobility (i.e. the surface diffusivity of the incoming species) are low [5]. As the deposition was performed at room temperature, this condition was fulfilled. Moreover, Pd has anisotropic elastic properties ($E_{100} = 75$ GPa and $E_{111} = 190$ GPa) which explains the anisotropic enlargement of the lattice.

3.1.2. Film 2

The Pd/Mg film deposited on a Ni substrate under an Ar atmosphere consists of a Mg layer of ∼300 nm covered by a Pd layer of ∼30 nm. As shown in Fig. 1b, the palladium diffraction peaks are clearly visible but a diffraction peak associated with Mg is also discernible at ca. 36.5°. The low intensity of the Mg peak compared to Pd peaks is related to the fact that only the outermost layer (i.e. ∼15 nm) is probed at a grazing angle of 2°. Pd and Mg crystallite sizes are about 10–15 and 30 nm, respectively. On the basis of the lattice parameters, the palladium layer does not display lattice deformations in contrast to that observed previously for a Pd film deposited on a coarse-grained Mg subtract (Fig. 1a). It may be related to the nanocrystalline characteristic of the Mg underlayer that may favour the adatom mobility upon the Pd film growth.

3.1.3. Film 3

The only difference with the previous two-layered Pd/Mg film deposition procedure is the nature of the gas in the PLD chamber (i.e. helium instead of argon). This has a strong influence on the film structure. Indeed, as seen in Fig. 1c, the Mg diffraction peaks are much more apparent in comparison to the XRD pattern of Pd/Mg film performed under argon (Fig. 1b) despite the same probed depth and the same amount of Pd and Mg deposited onto the substrate. No diffraction peaks ascribed to Mg–Pd alloys or solid solutions are detected. The crystallite sizes are ∼15 nm for palladium and ∼30 nm for magnesium. Depth profile XPS analyses show the presence of an extended Pd gradient in the Mg layer for the Pd/Mg film prepared in helium atmosphere in contrast to the sample prepared under argon displaying a sharp Pd/Mg interface as indicated in Fig. 2.

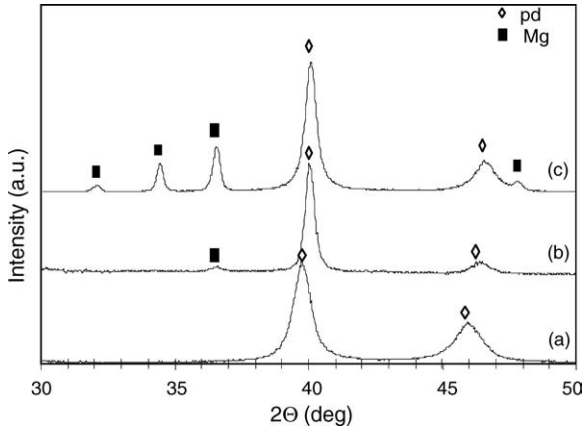

Fig. 1. XRD patterns (grazing angle of 2°) of (a) Pd film on a Mg substrate, (b) Pd/Mg film deposited on a Ni substrate under Ar, (c) Pd/Mg film deposited on a Ni substrate under He.

In addition, it must be noted that the presence of an inert gas in the PLD chamber is a key parameter to avoid the Mg oxidation during the deposition procedure. Comparable observation was made elsewhere for the synthesis of superconductor MgB_2 thin films by PLD [6,7]. The role of the inert gas in the decreasing amount of MgO is nevertheless not well-established. It is possible that fresh surface sites are quickly blocked by inert gas molecules due to the large number of inert gas molecules in the PLD chamber compared to the oxygen molecules and then, maybe, the oxygen molecules do not reach the surface before the next pulse comes. The role of inert gas in the decreasing of MgO can be also explained by alterations in the plume dynamics (e.g. ratio of neutral Mg versus ionized Mg) [6].

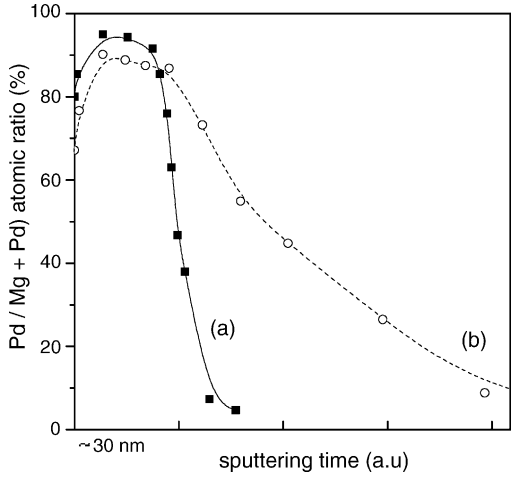

Fig. 2. Evolution of the Pd/(Mg + Pd) atomic ratio (%) as a function of the sputtering time from XPS analysis: (a) Pd/Mg film deposited on a Ni substrate under Ar, (b) Pd/Mg film deposited on a Ni substrate under He.

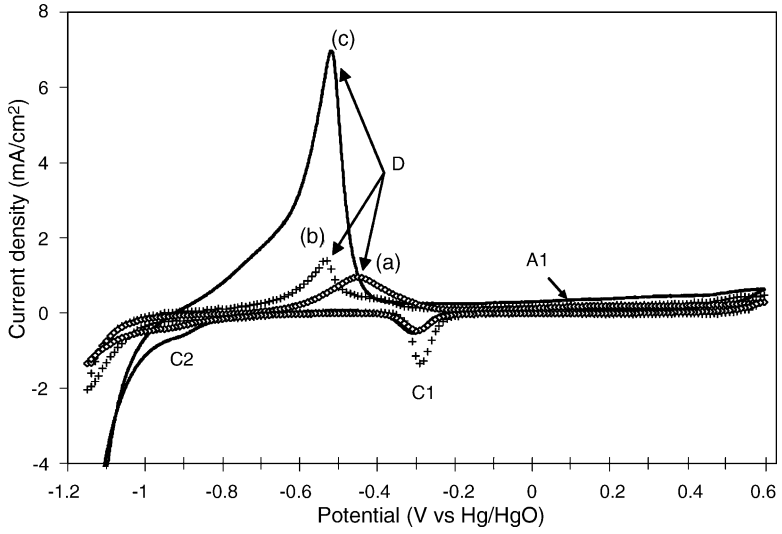

Fig. 3. Cyclic voltammograms in 1 M KOH at 50 mV/s of (a) Pd film on a Mg substrate, (b) Pd/Mg film deposited on a Ni substrate under Ar, (c) Pd/Mg film deposited on a Ni substrate under He.

3.2. Electrochemical behaviour

Curve a in Fig. 3 shows the cyclic voltammogram of the Pd film on a Mg substrate (film 1) performed in 1 M KOH at 50 mV s^{-1} between −1.15 and 0.6 V versus Hg/HgO. The broad anodic peak (labelled DH) at ca. −0.45 V is related to the desorption of hydrogen absorbed during the previous negative potential scan. An anodic wave (A1) coupled to the cathodic peak (C1) located at ca. −0.2 V are assigned to a Pd(II) oxide/hydroxide surface formation/reduction process. A cathodic wave (C2) assigned to hydrogen adsorption is observed at potentials around −0.9 V. The hydrogen evolution reaction (HER) occurs at potentials more negative than −0.9 V. The electrochemical response of the Pd film on a Mg substrate is very close to the one previously reported for Pd films deposited on a Ni substrate [8]. Moreover, the maximum H-solubility determined from the DH-peak charge after prolonged cathodic polarization is similar, i.e. the maximum H/Pd atomic ratio is ∼ 0.32 on Ni and Mg substrates. Thus, the simple coating of polycrystalline Mg with Pd does not allow the electrochemical hydriding/dehydridring of Mg at room temperature. It may be related to the presence of a native oxide layer on the Mg substrate acting as a barrier for hydrogen diffusion as well as the very low hydriding kinetics in polycrystalline Mg. It must be noted that the maximum H/Pd value for Pd film is lower than usually observed in bulk Pd (H/Pd atomic ratio ∼0.67). It could be related to the lattice anisotropic strain of the Pd film, inducing a broadening of the interstitial site energy distribution. The restriction of the volume expansion due to the substrate as well as the presence of grain boundaries in large proportion may have also an incidence on the hydrogen solubility [9].

Curve b in Fig. 3 presents the cyclic voltammogram of the Pd/Mg film deposited on a Ni substrate under argon pressure (film 2). The electrochemical response is basically the same as the one described before for Pd film on Mg substrate (curve a) but some differences appear. The C1-peak charge related to Pd oxides reduction is more important, which may reflect an increase of the film roughness. The DH peak related to H-desorption is shifted towards more negative potentials and a shoulder is discernable at ca. −0.4 V. Moreover, the anodic charge associated with the DH-peak is slightly higher than the maximum charge that can be attributed to the H-desorption reaction from the outermost Pd layer. A part of the DH-peak charge is therefore associated with H-desorption from the Mg layer. On the contrary to the Pd film on Mg substrate, Mg layer was prepared in-situ and thence the deleterious native MgO layer preventing hydrogen diffusion in Mg is not present at the Pd/Mg interface. Moreover, the Mg layer has a nanocrystalline structure which may favour the hydriding/dehydriding process. Nevertheless, the H-solubility in the Mg layer is very small (H/Mg atomic ratio <0.1) indicating that hydrogen in Mg phase is essentially located near the Pd/Mg interface. It can be explained by the fact that the MgH_2 layer formed at the Pd–Mg interface may act as a diffusion barrier for further hydriding in the Mg layer [10–12]. It should be noted that the deposition of an additional layer of Pd between the Ni substrate and the Mg layer (i.e. the formation of a three-layered Pd/Mg/Pd film) did not improve significantly the H-solubility into the film in contrast to that observed in Pd/Mg/Pd prepared by RF-magnetron sputtering [2]. Moreover, Pd/Mg film shows a rapid degradation upon electrochemical cycling due to the palladium layer peeling off/tearing as confirmed by SEM pictures done after tests (not shown). It can be explained by the stress induced at the Pd/Mg interface due to the film volume expansion accompanying the hydrogen absorption process.

Curve c in Fig. 3 presents the cyclic voltammogram of the Pd/Mg film deposited under He atmosphere on Ni substrate (film 3). The DH-peak charge related the H-desorption is obviously much more important compared to the one observed previously with Pd/Mg film deposited under Ar (curve b)

despite their similar thickness (∼300 nm). It may be related to the presence of a large number of Pd–Mg interfaces through the creation of an extended Pd–Mg mixing region under He atmosphere as shown previously. Moreover, the film displays a high cycling stability (200 complete absorption/desorption cycles were performed with a capacity loss per cycle as low as ∼0.4%). This indicates that such hydriding film morphology may be suitable for Ni-MH microbatteries.

References

[1] K. Higuchi, H. Kajioka, K. Toiyama, H. Fujii, S. Orimo, Y. Kikuchi, J. Alloys Compd. 293-295 (1999) 484.
[2] K. Higuchi, K. Yamamoto, H. Kajioka, K. Toiyama, M. Honda, S. Orimo, H. Fujii, J. Alloys Compd. 330-332 (2002) 526.
[3] H. Fujii, K. Higuchi, K. Yamamoto, H. Kajioka, S. Orimo, K. Toiyama, Mater. Trans. 43 (2002) 2721.
[4] D.B. Chrisey, G.K. Hubler, Pulsed Laser Deposition of thin films, John Wiley & Sons, New York, 1994.
[5] W.D. Nix, B.M. Clemens, J. Mater. Res. 14 (1999) 3467.
[6] V. Ferrando, S. Amoruso, E. Bellingeri, R. Bruzzese, P. Manfrinetti, R. Velotta, X. Wang, C. Ferdeghini, Supercond. Sci. Technol. 16 (2003) 241.
[7] A. Brinkman, D. Mijatovic, G. Rijnders, V. Leca, H.J.H. Smilde, I. Oomen, A.A. Golubov, F. Roesthuis, S. Harkema, H. Hilgenkamp, D.H.A. Blank, H. Rogalla, Phys. C 353 (2001) 1.
[8] J. Paillier, L. Roue, J. Electrochem. Soc. 151 (2005) E1.
[9] A. Pundt, Adv. Eng. Mater. 6 (2004) 11.
[10] A. Krozer, B. Kasemo, J. Vac. Sci. Technol. A 5 (1987) 1003.
[11] J. Ryden, B. Hjorvarsson, T. Ericsson, E. Karlsson, A. Krozer, B. Kasemo, J. Less-Common Met. 152 (1989) 295.
[12] A. Krozer, B. Kasemo, J. Less-Common Met. 160 (1990) 323.